Non-linear Control of a Piezoelectric Two Stage Servovalve

Johan Persson, Andrew Plummer, Chris Bowen and Phil Elliott*

Department of Mechanical Engineering, University of Bath, Bath, United Kingdom
E-mail: ljp46@bath.ac.uk, A.R.Plummer@bath.ac.uk, C.R.Bowen@bath.ac.uk
* Moog Aircraft Group, Moog Controls, Ashchurch, Tewkesbury, United Kingdom
E-mail: pelliott2@moog.com

Abstract

This paper describes an algorithm to control a two stage hydraulic servovalve designed for aerospace applications. The valve has a piezoelectric ring bender actuating a first stage spool with a significant amount of overlap to reduce internal leakage. The piezoelectric ring bender is a less complex and lighter alternative to a conventional torque motor. The second stage has electrical instead of the conventional mechanical feedback. The control algorithm includes compensation for the first stage spool overlap, piezoelectric hysteresis compensation and a feed forward term. The hysteresis compensation is based on a relatively simple Bouc-Wen hysteresis model that is able to significantly reduce the amount of first stage hysteresis. The overlap compensation, increasing the gain in the overlap region, reduces the impact of amplitude change and increases performance. It can also reduce any asymmetry in the system. The controller has a superior performance compared to a PI controller, as demonstrated experimentally using step and frequency responses.

Keywords: piezoelectric actuator, two-stage servovalve, spool, hysteresis compensation.

1 Introduction and Valve Prototype

This paper describes a control algorithm used to control the position the main stage in a two stage servovalve designed for aerospace flight control applications. It has a piezoelectric ring bender actuating the pilot stage spool and a second stage spool with electrical feedback.

A two-stage servovalve converts an electrical signal into the position of a fluid-metering spool via a hydraulic amplification stage [1]. Such a servovalve is usually used to control flow to the hydraulic actuator where high performance motion control is required.

In a typical single-aisle airliner there are approximately 40 hydraulic servovalves, which are the key control component in electrohydraulic actuation for primary flight control, landing gear deployment, on-ground braking and steering. Key drivers for new aerospace hydraulic servovalve designs is to reduce weight, reduce manufacturing cost, and improve efficiency through reduced internal leakage. For example, by reducing the internal leakage of servovalve approximately 2200 USD per valve per year of fuel cost could be saved by the airline companies [2]. To reduce the internal leakage a small spool with significant overlap was used for the pilot stage.

In a conventional valve, the first (or pilot) stage refers to the torque motor and either nozzle-flapper, jet pipe or deflector jet amplifier, and provides the actuation to move the main spool (second stage). Torque motors can be time-consuming and expensive to set-up, requiring significant manual intervention [3]. If not adjusted precisely the first stage amplifier may not provide stable operation, and there is a continual flow loss (and power loss) through the nozzles or jet. An alternative approach is required providing a more cost effective, reliable and which is amenable to automated manufacture.

Smart materials, and in particular piezoelectric ceramics, are a possible alternative potentially providing high forces and fast response times [4], [5]. Stack and bending actuators have extensively been researched [6]. The relatively new multilayer three wire piezoelectric ring bender is a type of bending actuator, which is a flat annular disc that deforms in a concave or convex fashion depending on the polarity of the applied voltage, see Figure 1 (c) [6], [7]. Such an actuator configuration has been chosen for first stage actuation since it exhibits a greater displacement than a stack actuator of the same mass, and an increase in stiffness in comparison to similar size rectangular bimorph type bender, resulting in a larger force output.

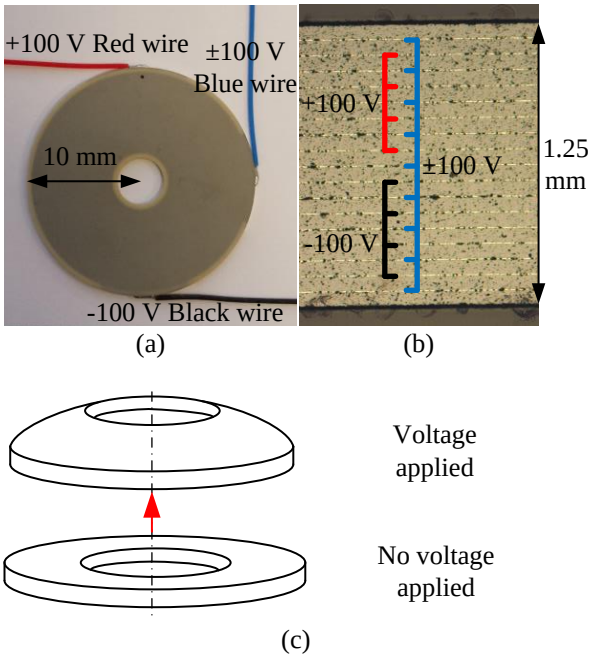

Figure 1. (a) Noliac piezoelectric ring bender (b) Microscopic section of a piezoelectric ring bender (c) Piezoelectric ring bender deformation

A Noliac CMBR08 multilayer, three wire design, piezoelectric ring bender is used for actuating the first stage in the prototype valve. The piezoelectric ring bender has a 40mm diameter and 1.2mm thickness, a free displacement of ±115µm and a blocking force of ±39N. Figure 1 (a) shows the ring bender with its three wire electrical connection. The bender is made up of multiple 67µm thick lead zirconium titanate (PZT) piezoelectric ceramic layers. To apply the necessary electric field across the piezoelectric ceramic and thereby actuate the device, silver palladium electrodes are located between each layer; as can be seen from the light lines in Figure 1 (b). In order to deflect the ring bender in both directions the electrodes are combined into three groups, as shown in Figure 1 (b) [8].

The concept for the first stage is to use the ring bender to actuate a small spool, see Figure 2, with significant overlap to reduce the internal leakage. The piezoelectric ring bender moves the spool to control the flow to the second stage.

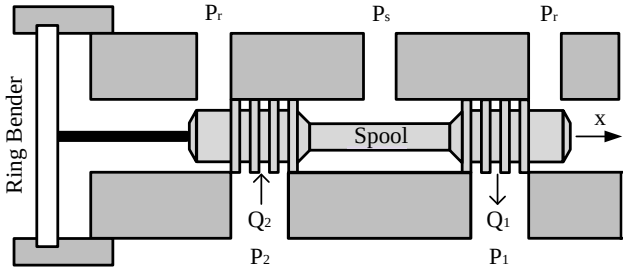

Figure 2. First stage concept.

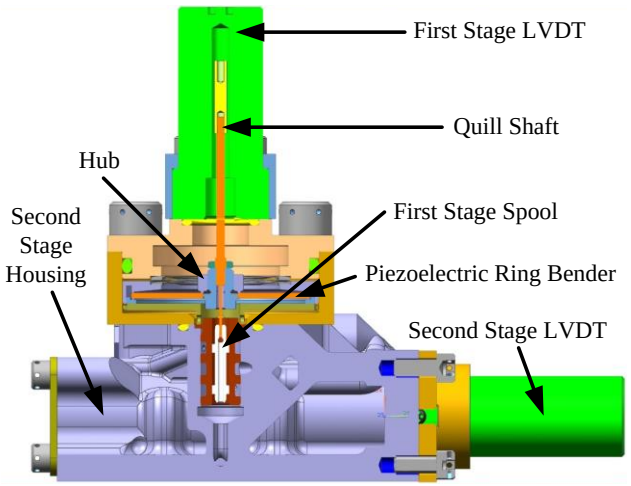

Figure 3. Cross section of the pilot stage.

Electrical second stage feedback allows a sophisticated digital controller to be implemented and will be more effective to counteract disturbances [9], compared to valves with mechanical feedback.

The piezoelectric actuated valve prototype was built and tested on a dedicated test bench. The second stage titanium alloy spool housing was made through AM, which, as discussed earlier, enable a greater design freedom. Figure 3 shows a cross section of the pilot stage, where the first stage spool, piezoelectric ring bender and the LVDT's to obtain first and second stage position can be seen. A photograph of the valve and the AM housing is shown in Figure 4. A circuit diagram of the system can be seen in Figure 5.

This paper presents a control strategy for compensating the hysteresis of the piezoelectric ring bender, without using additional sensors (such as pilot stage position feedback), which add weight, cost and complexity to the valve. The first stage LVDT in the prototype will merely be used to monitor the performance of the piezoelectric ring bender and first stage spool, and not used for control

The influence of a reduction of first stage piezoelectric hysteresis on the second stage positioning performance was studied. The study also includes compensation for the first stage spool overlap and implementation of a feed forward term to increase the second stage performance.

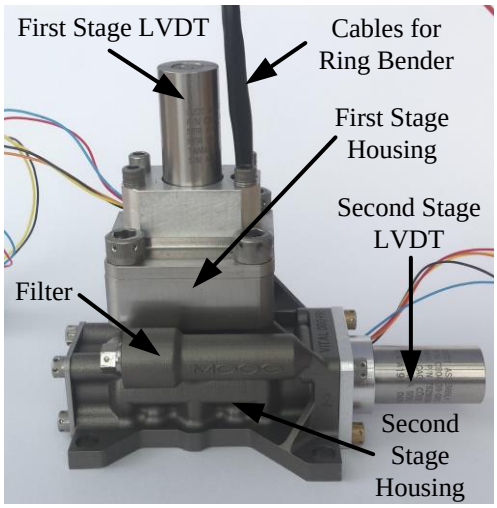

Figure 4. Photograph of the valve tested.

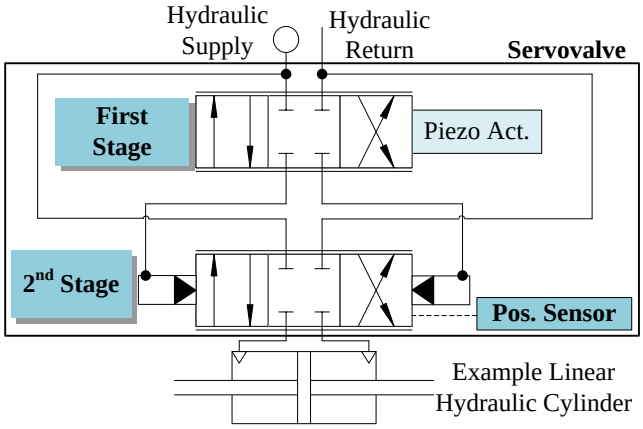

Figure 5. Internal servovalve circuit.

2 Controller Design

In traditional two stage servovalves with mechanical feedback and torque motor the steady state spool position is proportional to the electrical input current to the torque motor [10] [11]. This is achieved by the feedback spring exerting a feedback torque on the torque motor proportional to spool position.

The controller platform used for this investigation was an xPC system where a Simulink model is coded in real-time to control the pilot and main stage spool. A circuit diagram of the control setup can be seen in Figure 6. An amplifier was needed to drive the piezoelectric ring bender. The controller algorithm provides low control voltage, u_4, to the amplifier the controls the first stage piezoelectric ring bender. The system was setup to record the first and second stage spool positions as well as amplifier voltage.

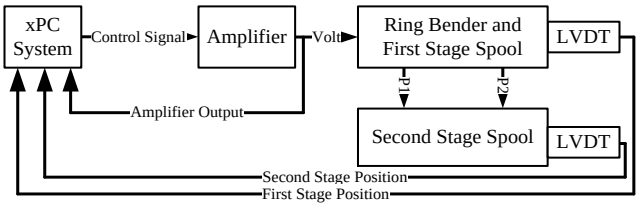

Figure 6. Circuit diagram of the control setup

A proportional-Integral (PI) controller is a common feedback control algorithm using a conventional Proportional, K_p, and Integral, K_I, gains as can be seen in Figure 7. In this case, with piezoelectric hysteresis and a significant amount of first stage spool overlap this is not sufficient as will be described later.

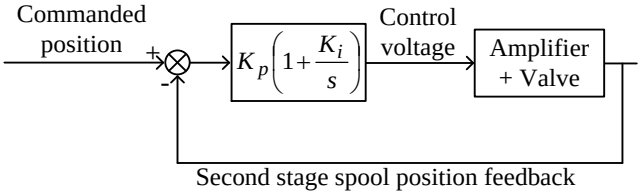

Figure 7. PI control loop

The control algorithm proposed in this paper, see Figure 8, includes overlap compensation, hysteresis compensation and command velocity feed forward terms. The hysteresis and overlap compensation are intended to make the system more linear and the feed forward loop is to make the response faster. The controller block diagram is shown in Figure 8.

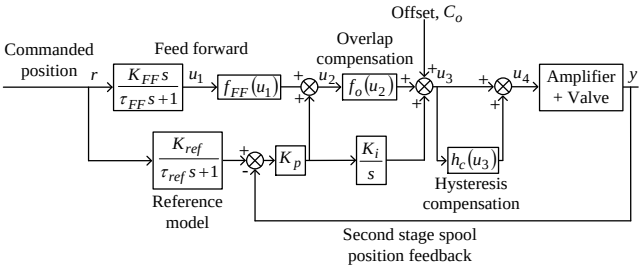

Figure 8. Proposed control algorithm.

2.1 Hysteresis Compensation

Previously in inverse hysteresis model of the more complicated Prandtl-Ishinskii model has been used for hysteresis compensation of a piezoelectric ring bender [12]. The Bouc-Wen model has been tested in a similar fashion as discussed in this paper, but using the model as a feedback, to eliminate the hysteresis of a rectangular piezoelectric bender [13]. However, that work no dynamic responses were being investigated.

The hysteresis compensation used for this work is based on a Bouc-Wen hysteresis model [14], which is a relatively simple model and also simple to implement into the control algorithm [13]. The Bouc-Wen model has three dimensionless tuning parameters, as seen in eq. (1). The

hysteresis term n is the derivation away from the linear response, u_3 is the demanded voltage from the controller (voltage after the overlap compensation and integral gain) and α, β and γ are the three dimensionless tuning parameters. Figure 9 shows an experimental hysteresis loop and a simulated hysteresis loop where n is added to the linear response. It can be seen that the hysteresis model matches the experimental data. In the compensator, n times a scaling factor, is added to the control voltage, as can be seen in Figure 8. The scaling factor, K_h see equation (2) is needed to restore the correct linear gain.

$$\dot{n} = \alpha \dot{u}_3 - \beta|\dot{u}_3|n - \gamma \dot{u}_3|n| \qquad (1)$$

$$h_c(u_3) = K_h n \qquad (2)$$

Figure 10 shows experimental hysteresis loops with and without hysteresis compensation and as can be seen the hysteresis is significantly reduced. The three tuning parameters values can be seen in Table 1.

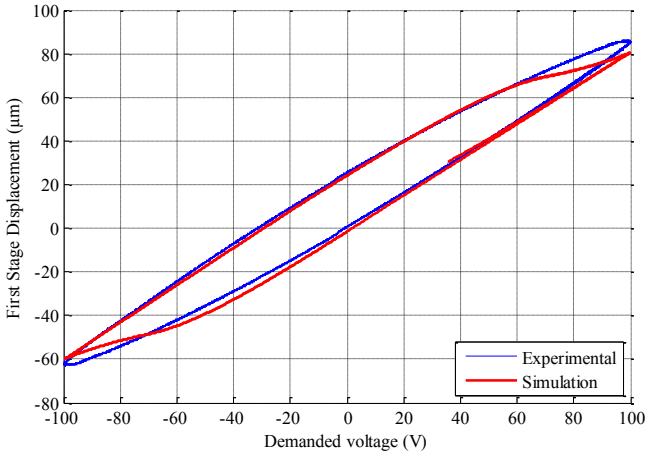

Figure 9. Experimental hysteresis loop vs simulated hysteresis loop.

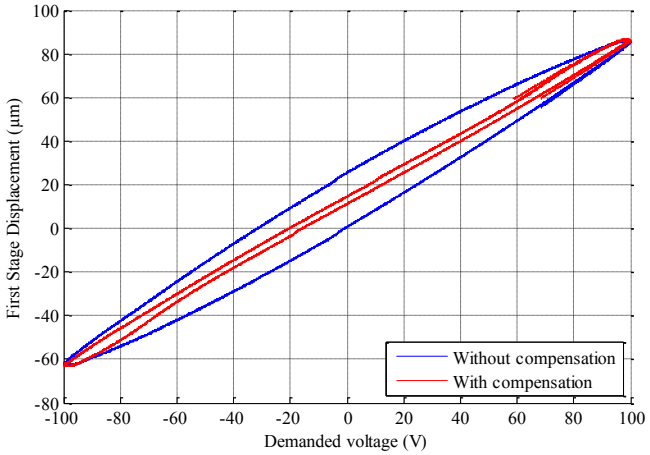

Figure 10. Experimental hysteresis compensation loop.

2.2 Overlap Compensation

The first stage spool is closed center with a significant amount of overlap, ~20µm, to reduce the internal leakage. A closed center arrangement will result in a 'dead-band' where very little flow is passing to the second stage in the overlap region [15], as can be seen in Figure 11.

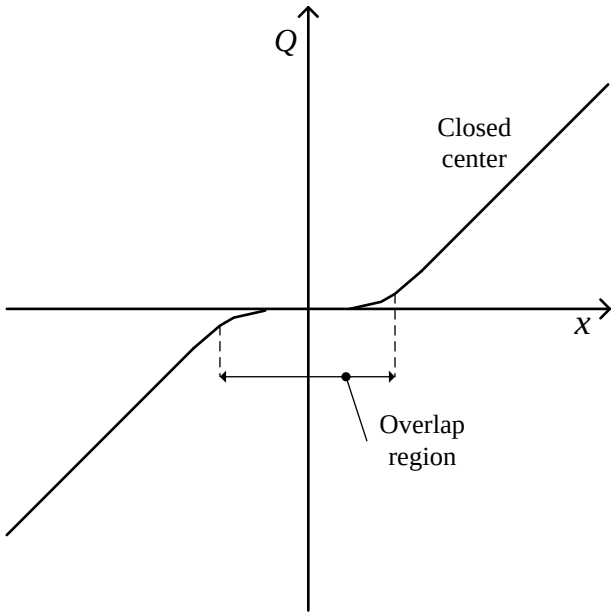

Figure 11. Flow gain for closed center spool.

To be able to linearize the system this dead-band has to be compensated for. The overlap compensation was implemented as a look-up table where a higher gain was implemented while the first stage spool was in the overlap region (f_o), see Figure 12. Figure 13 shows the measured second stage velocity versus the first stage position. The overlap compensation also compensated for the asymmetry and the offset, as can be observed in Figure 13. The offset between the electrical null for the piezoelectric ring bender and the hydraulic null of the first stage spool, seen in Figure 13, is compensated by an offset term C_o (Figure 8). In Figure 13 a small lag between the first stage position and second stage velocity can be observed.

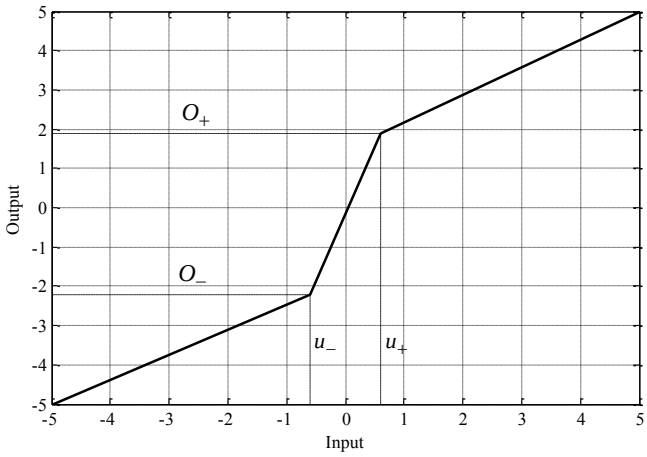

Figure 12. Overlap compensation look-up table.

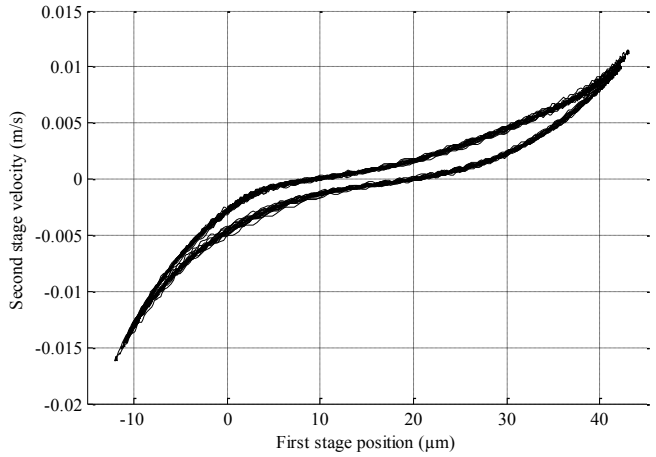

Figure 13. Flow from the first to second stage.

2.3 Command Velocity Feedforward

The feedforward command velocity is estimated by differential position filtered by a first order lag a reference model, as can be seen in Figure 8. The feed forward will speed up the transient response, which generally means increasing the bandwidth of the system [16]. The feedforward loop also compensates for velocity asymmetry in the system. The asymmetry is due to the null offset in the valve coupled to the non-linear stiffness of the piezoelectric ring bender mounting. The function $f_{FF}(u_1)$ term is a lookup table as shown below:

$$f_{FF}(u_1) = 1.4u_1 \text{ if } u_1 \geq 0$$

$$f_{FF}(u_1) = u_1 \text{ if } u_1 < 0$$

A reference model is included as a prediction of the response of the system to the feedforward path. The feedback control thus only ad on the error between the actual spool position and the predicted position. This error can also thought of as a disturbance observer.

Table 1. Parameter table.

	Parameter	Value
Hysteresis compensation parameters	α, Hystereis tuning parameter	0.0017 (-)
	β, Hystereis tuning parameter	0.00065 (-)
	γ, Hystereis tuning parameter	0.0015 (-)
	K_h, Hysteresis scaling factor	0.87 (-)
Overlap compensation parameters	O_+, Positive overlap compensation output	1.9 V
	O_-, Negative overlap compensation output	-2.2 V
	u_+, Positive overlap compensation input	0.6 V
	u_-, Negative overlap compensation input	-0.6 V
Feed forward loop parameters	K_{FF}, Feedforward term gain	0.00005 $V/(\mu m/s)$
	K_{ref}, Reference model gain	1 (-)
	τ_{FF}, Feedforward term lag	0.0015 (-)
	τ_{ref}, Reference model lag	0.003 (-)
Controller Settings	K_p, Proportional gain for the non-linear controller	0.012 $V/\mu m$
	K_i, Integral gain for the non-linear controller	200 (-)
	K_{p1}, Proportional gain for PI2	0.05 (-)
	K_{p2}, Proportional gain for PI2	0.03 (-)
	K_{i1}, Integral gain for PI1	1 (-)
	K_{i2}, Integral gain for PI2	1 (-)
	C_o, Null offset comensation	0.25 V

3 Results

The valve prototype with the proposed control algorithm has been tested. The effect of the different controller parts were compared. Four different controller arrangements were tested:

- Complete controller (FF+OC+HC)
- Overlap compensation (OC) and hysteresis compensation (HC)
- Overlap compensation (OC) and feed forward (FF)

- Only overlap compensation (OC).

In all cases the proportional and integral gain are unchanged. Two different step responses sizes, 60µm and 120µm, were tested as well as a 30µm amplitude frequency response. The new controller is compared to a conventional PI controller at the end of this section.
All tests were performed at 200 bar and at a temperature of about 39±1.5°C.
Figure 14 shows the 60µm step response and Figure 15 shows the 120µm step response. The rise time (0-90%) and the settling time (±5%) for both amplitudes can be seen in Table 2 and Table 3.
By only compensating for the overlap the rise time is 8.2ms for a 60µm step and 7.3 for a 120µm step size. The settling time for 120µm step was 57.6ms and was able to get within ±5% for the 60µm step. By having the overlap compensation and hysteresis compensation the response is quicker, but the device also experiences more overshoot. By having the overlap compensation and a feed forward term the response was even further improved. Rise time of 10.3ms and settling time of 19.9ms for 60µm step and 4.9ms and settling time of 5.2ms for a 120µm step size. The complete experimental controller had the overall fastest response with 4.6ms rise time and 15.7ms (8ms slower than with only overlap compensation and feed forward term) for a 60µm step and 4.3ms rise time and 4.8ms settling time for 120µm step.
The average difference between the commanded position and the actual position is 5.6µm for a 60µm step and 7.7µm for the controller without the hysteresis (OC+FF). This can be compared to the complete controller that has a difference of 4µm for 60µm step and 6.1µm for 120µm step.

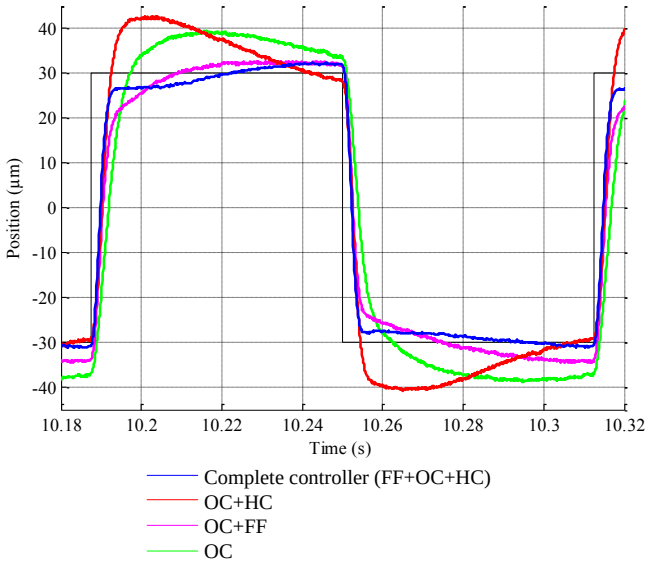

Figure 14. 60µm step response results.

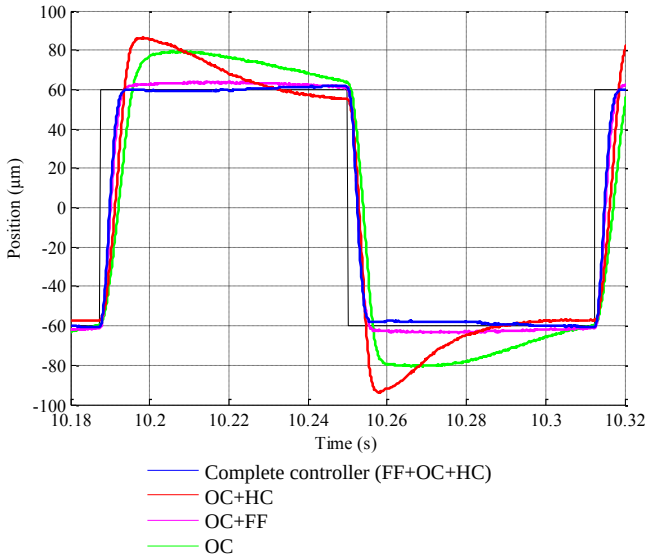

Figure 15. 120µm step response results.

Table 2. 60µm step response results with different combinations of overlap compensation (OC), feed forward (FF) and hysteresis compensation (HC).

60µm Step	**Rise time (0-90%)**	**Settling time (±5%)**
Complete controller (FF+OC+HC)	4.6ms	15.7ms
OC+HC	4.5ms	44.6ms
OC+FF	10.3ms	14.9ms
OC	8.2ms	>62.5ms

Table 3. 120µm step response results with different combinations of overlap compensation (OC), feed forward (FF) and hysteresis compensation (HC).

120µm Step	**Rise time (0-90%)**	**Settling time (±5%)**
Complete controller (FF+OC+HC)	4.3ms	4.8ms
OC+HC	5.7ms	35.8ms
OC+FF	4.9ms	5.2ms
OC	7.3ms	57.6ms

A frequency response test was completed with an amplitude of 30µm, see Figure 16. It can be seen that in the system where the feed forward loop is included both the magnitude and phase lag first decreases then increases again. This is most likely due to the increase in gain within the first stage overlap region, as the control voltage starts to increase.
It can also be seen in Figure 16 that the setup with overlap compensation and hysteresis compensation (without feedforward) has a better performance than the complete system until around 50 Hz for the magnitude and 30 Hz for the phase after those frequencies the complete setup performs

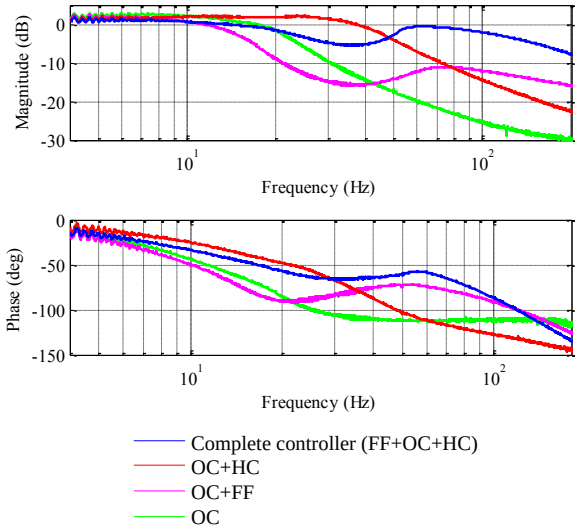

Figure 16. Frequency response results, 30µm amplitude.

The complete non-linear controller was compared to a well-adjusted conventional PI controller algorithm. Responses to steps of 60µm and 120µm were measure as well as a 30µm amplitude frequency response. Two different PI setups were tested, one was tuned for a square wave amplitude of 30µm amplitude (60µm step, PI1) and the second for a 60µm amplitude (120µm step, PI2).

As can be seen in Figure 17, 60µm step, and Figure 18, 120µm step, that for the same PI controller for the different amplitudes significantly different results will be obtained. It can also be observed that the proposed non-linear control algorithm is the better controller when it comes to rise time and settling time, as can be seen in Table 4 and Table 5 as well as being less effected by the amplitude change. The PI controller setup for a 30µm amplitude (60µm step) it did not reach within ±5% of the step within 62.2ms in either case.

Due to the large overlap of the first stage spool it is essential to obtain a control algorithm to compensate for this. It is important to be able to adjust for any nonlinearities within the system. It this system it is believed that the mounting creates an asymmetry in the results.

This is adjusted by having a different gains in each direction. Variation and asymmetry in the results has been observed, which is believed to be due to the temperature change. The change in stiffness of the mounting due to temperature changed is likely case of the asymmetry seen.

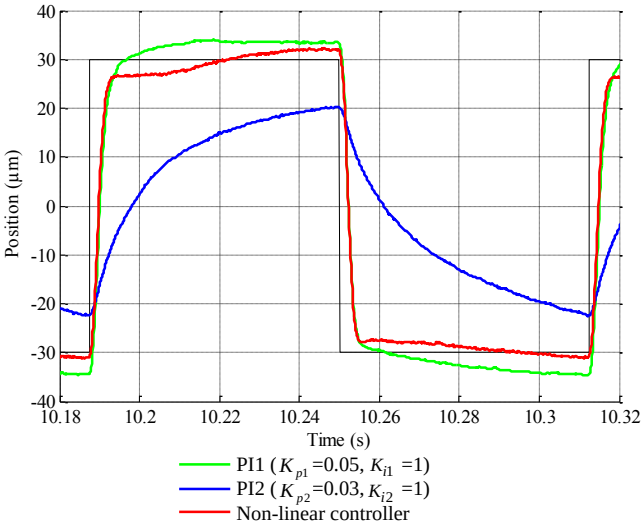

Figure 17. 60µm step, PI setup vs complete non-linear control algorithm.

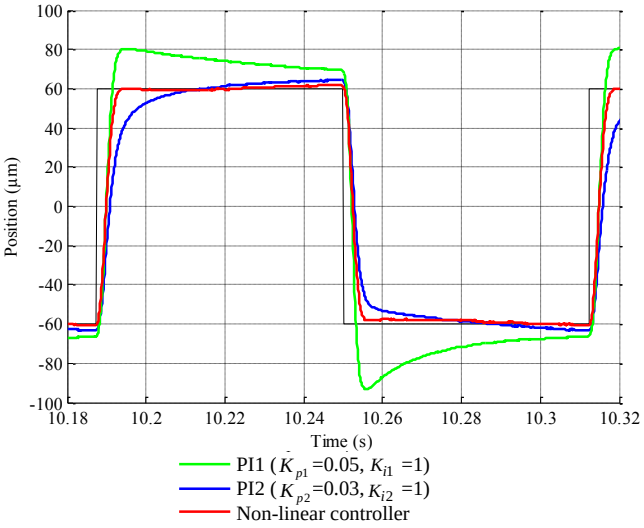

Figure 18. 120µm step, PI setup vs complete non-linear control algorithm.

Table 4. PI controller, 60µm step response.

60µm Step	**Rise time (0-90%)**	**Settling time (±5%)**
PI1 ($K_{p1}=0.05$ **,** $K_{i1}=1$**)**	5.2ms	>62.5ms
PI2 ($K_{p2}=0.03$ **,** $K_{i2}=1$**)**	>62.5ms	>62.5ms
Non-linear controller	4.6ms	15.7ms

Table 5. PI controller, 120µm step response.

120µm Step	**Rise time (0-90%)**	**Settling time (±5%)**
PI1 ($K_{p1}=0.05$ **,** $K_{i1}=1$**)**	3.7ms	>62.5
PI2 ($K_{p2}=0.03$ **,** $K_{i2}=1$**)**	9.4ms	14ms
Non-linear controller	4.3ms	4.8ms

A frequency response was completed for the two PI controllers and the non-linear controller, see Figure 19. It can be seen that the non-linear controller gives a better dynamic response particular in terms of magnitude throughout the frequency range. Note that the low frequency phase lag and alternation evident in the PI controller response is due to the hysteresis.

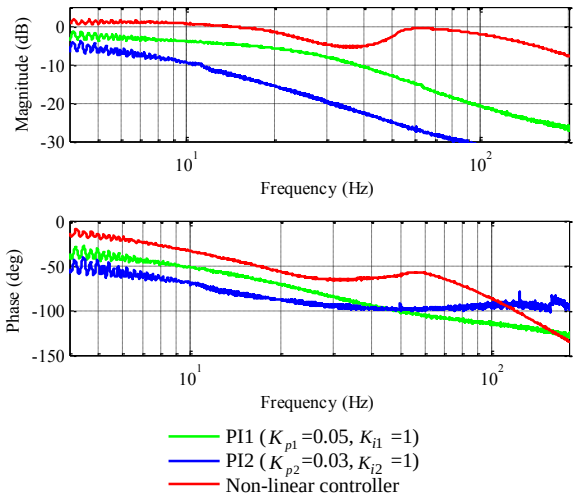

Figure 19. Frequency response conventional PI controller vs Experimental non-linear controller.

4 Conclusion

From this investigation there are several conclusions that can be drawn. A conventional PI controller is sensitive to amplitude changes, due to the lack of compensating for the first stage overlap. A higher gain in the first stage spool overlap region is essential to increase performance and be less sensitive to amplitude changes. First stage hysteresis compensation improved the response of the second stage performance. The feed forward control loop have the effect on the frequency response in the way that both the magnitude and phase will start to drop and then increase again. The complete experimental control algorithm provides the fastest response. It is shown that the non-linear controller significantly outperforms two PI controller, which span the range of plausible proportional gain values.

Work currently ongoing:

i. Reliability of piezoelectric ring benders in aerospace hydraulic fluid.
ii. Mounting optimization of piezoelectric ring bender.

Nomenclature

Designation	Denotation	Unit
n	Hysteresis nonlinear term	V
Q	Flow	m^3/s
x	Position	μm
r	Commanded position	μm
u_i	Control signal at different places in the non-linear control algorithm	-
y	Final control voltage	V
P	Pressure	bar
FF	Feed forward loop	-
HC	Hysteresis compensation	-
OC	Overlap compensation	-

Acknowledgment

The authors would like to thank Moog Aircraft Group, Renishaw and Innovate UK for supporting this research. Ownership of Intellectual Property described in this work is detailed in collaboration agreements for VITAL IUK project 17413-117299 and Moog-Bath PhD Studentship Agreement of 5/9/15.

References

[1] Moog, “Servo Valves,” 2017. [Online]. Available: http://www.servovalve.com/. [Accessed: 12-Jan-2017].

[2] Moog, “Servovalve Leakage Fuel Costs (Moog Internal Report),” 2012.

[3] D. K. Sangiah, A. R. Plummer, C. R. Bowen, and P. Guerrier, “A novel piezohydraulic aerospace servovalve. Part 1: design and modelling,” *Proc. Inst. Mech. Eng. Part I J. Syst. Control Eng.*, vol. 227, no. 4, pp. 371–389, 2013.

[4] C. Mangeot, B. Anderssen, and R. Hilditch, “New Actuators for Aerospace,” Kvistgaard, 2008.

[5] R. Le Letty, F. Claeyssen, F. Barrillot, and N. Lhermet, “Amplified Piezoelectric Actuators for Aerospace Applications,” *AMAS Work. Smart Mater. Struct.*, pp. 51–63, 2003.

[6] M. J. F. Bertin, C. R. Bowen, A. R. Plummer, and D. N. Johnston, “An Investigation of Piezoelectric Ring Benders and Their Potential for Actuating Servo Valves,” in *Proceedings of the Bath/ASME Symposium on Fluid Power and Motion Control*, 2014, p. 6.

[7] Noliac, “Ring Benders,” 2015. [Online]. Available: www.noliac.com. [Accessed: 01-Dec-2015].

[8] J. Persson, C. R. Bowen, A. R. Plummer, and P. L. Elliott, “Dynamic Modelling and Performance of a Two Stage Piezoelectric Servovalve,” in *Proceedings of the ASME 2016 9th FPNI Ph.D Symposium on Fluid Power*, 2017, pp. 1–10.

[9] J. C. Jones and T. S. Manager, “Development in Design of Electrohydraulic Control Valves From Their Initial Design Concept to Present Day Design And Applications.” Moog Australia PTY LTD., pp. 1–19, 1997.

[10] Moog, “Electrohydraulic Valves... A Technical Look.”

[11] Moog, “Type 26 Single Inlet Flow Control Servovalves,” 2011.

[12] F. Stefanski, B. Minorowicz, J. Persson, A. Plummer, and C. Bowen, “Non-linear control of a hydraulic piezo-valve using a generalised Prandtl – Ishlinskii hysteresis model,” *Mech. Syst. Signal Process.*, vol. 82, pp. 412–431, 2017.

[13] M. Rakotondrabe, “Bouc – Wen Modeling and Inverse Multiplicative Structure Actuators to Compensate Hysteresis Nonlinearity in Piezoelectric Actuators,” vol. 8, no. 2, pp. 428–431, 2011.

[14] D. K. Sangiah, “Fluid Metering Using Active Materials,” University of Bath, 2011.

[15] K.-E. Rydberg, “Hydraulic Servo Systems.” Linköpings Universitet, Linköping, 2008.

[16] Parker Hannifin - Electromechanical Automation Div., “Fundamentals of Servo Motion Control.”